

# Perfect domination in regular grid graphs

ITALO J. DEJTER  
University of Puerto Rico  
Rio Piedras, PR 00931-3355  
ijdejter@uprrp.edu

## Abstract

We show there is an uncountable number of parallel total perfect codes in the integer lattice graph  $\Lambda$  of  $\mathbf{R}^2$ . In contrast, there is just one 1-perfect code in  $\Lambda$  and one total perfect code in  $\Lambda$  restricting to total perfect codes of rectangular grid graphs (yielding an asymmetric, Penrose, tiling of the plane). We characterize all cycle products  $C_m \times C_n$  with parallel total perfect codes, and the  $d$ -perfect and total perfect code partitions of  $\Lambda$  and  $C_m \times C_n$ , the former having as quotient graph the undirected Cayley graphs of  $\mathbf{Z}_{2d^2+2d+1}$  with generator set  $\{1, 2d^2\}$ . For  $r > 1$ , generalization for 1-perfect codes is provided in the integer lattice of  $\mathbf{R}^r$  and in the products of  $r$  cycles, with partition quotient graph  $K_{2r+1}$  taken as the undirected Cayley graph of  $\mathbf{Z}_{2r+1}$  with generator set  $\{1, \dots, r\}$ .

## 1 Introduction

As in [11], a vertex subset  $S$  in a graph  $G$  is said to be a *perfect dominating set* (PDS) in  $G$  if each vertex of the complementary graph  $G \setminus S$  of  $S$  in  $G$  is adjacent to just one element of  $S$ . In that case, if the induced components of  $S$  are 1-cubes, (respectively 0-cubes), then  $S$  is said to be a *total perfect code* [7], (respectively a *1-perfect code* [8], or *efficient dominating set* [2]).

vspace\*5mm

The NP-completeness of finding a 1-perfect code in  $G$  and that of finding a minimal PDS in a planar graph were established respectively in [2, 8] and in Sections 3 and 4 of [6], even if its induced components are  $i$ -cubes with  $i \leq 1$ .

The *integer lattice graph*  $\Lambda$  of  $\mathbf{R}^2$  is the graph with vertex set  $\{(i, j) : i, j \in \mathbf{Z}\}$  and such that any two vertices in  $\Lambda$  are adjacent if and only if their Euclidean distance is 1.  $\Lambda$  and its subgraphs are represented orthogonally, their vertical paths from left to right for increasing indices  $i = 0, 1, 2, \dots, m-1$  and its horizontal paths downward for increasing indices  $j = 0, 1, 2, \dots, n-1$ . If a total perfect code in  $\Lambda$  has its induced components as pairwise parallel 1-cubes in  $\Lambda$ , then it is said to be *parallel*.

We represent a perfect dominating set  $S$  in  $\Lambda$  by setting the vertices of  $S$  as black dots at their locations and by tracing only the edges between vertices in  $\Lambda \setminus S$  (by means of unit-length solid segments), thus avoiding (or deleting) those edges in  $\Lambda$

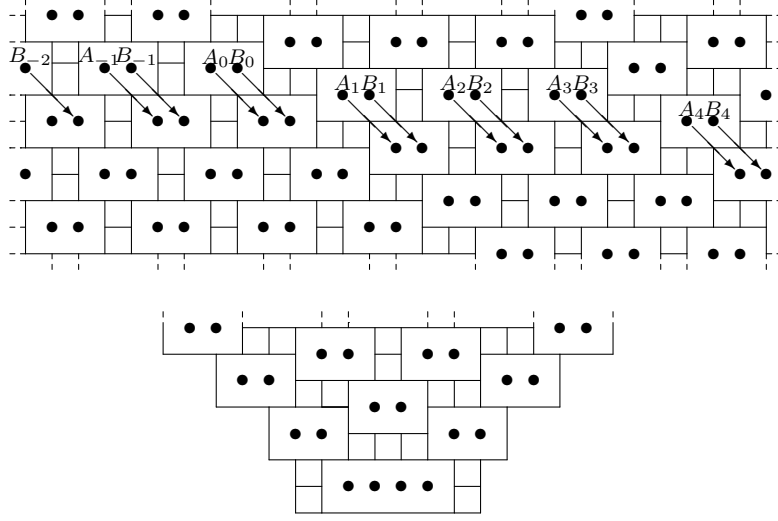


Figure 1: Illustrations for Theorem 1

incident to  $S$ . This way, we represent not only  $S$  but also  $\Lambda \setminus S$ , as in Figure 1, that accompanies Theorem 1. Notice that  $G \setminus S$  is 3-regular, for any PDS  $S$  in a 4-regular graph  $G$ , like  $G = \Lambda$ .

We show in Section 2 that there is no algorithmic characterization of parallel total perfect codes in  $\Lambda$ . In fact, there is an uncountable number of such codes, in one-to-one correspondence with the doubly infinite binary sequences. This allows to characterize, in Section 3, all cycle products  $C_m \times C_n$  in which parallel total perfect codes exist, and in Sections 4 and 5, the  $d$ -perfect and total perfect code partitions of  $\Lambda$  and  $C_m \times C_n$ . We also show that the quotient graphs of these  $d$ -perfect code partitions are Cayley graphs of  $\mathbf{Z}_{2d^2+2d+1}$  with generator sets  $\{1, 2d^2\}$ . In contrast with the mentioned uncountability, seen as one of perfect dominating sets, not only there is just one 1-perfect code in  $\Lambda$  but, as a result of a characterization of grid graphs containing total perfect codes due to Klostermeyer and Goldwasser, there exists only one total perfect code in  $\Lambda$  that restricts to total perfect codes of rectangular grid graphs, its complementary graph in  $\Lambda$  yielding an asymmetric tiling of the plane, like the Penrose tiling, (Section 6). Section 7 considers some special cases, including a correction to a result of [9]. In Section 8, the generalization of the results for 1-perfect codes is provided in dimensions  $r > 1$ , with partition quotient graph  $K_{2r+1}$  as undirected Cayley graph of  $\mathbf{Z}_{2r+1}$  with generator set  $\{1, \dots, r\}$ .

## 2 Total perfect codes in $\Lambda$

**Theorem 1** *The family of PDSs in  $\Lambda$  whose induced components are parallel, horizontal, 1-cubes is in one-to-one correspondence with the set of doubly infinite  $\{0, 1\}$ -sequences.*

*Proof.* Let  $(\dots, a_{-i}, \dots, a_0, \dots, a_i, \dots)$  be a doubly infinite  $\{0, 1\}$ -sequence.

Define vertices  $A_n, B_n$  in  $\Lambda$  by means of

$$A_{-n} = \Sigma_{i=-1}^{-n} - (4 + a_i, a_i), \quad A_0 = (0, 0), \quad A_n = \Sigma_{i=1}^n (4 + a_i, a_i),$$

for  $n > 0$ ; and  $B_n = A_n + (1, 0)$ , for  $n \in \mathbf{Z}$ . Then,

$$\cup_{j=-\infty}^{\infty} s^j(\cup_{i=-\infty}^{\infty} \{A_i, B_i\})$$

is a PDS in  $\Lambda$ , where  $s^j(x, y) = (x + 2j, y + 2j)$ , with  $j \in \mathbf{Z}$ . This yields the claimed correspondence. For example,

$$(\dots, a_{-2}, a_{-1}, a_0, a_1, a_2, a_3, a_4, a_5, \dots) = (\dots, 0, 0, 1, 0, 0, 1, 1, \dots)$$

is sent into a PDS  $S$  as partially represented on the upper part of Figure 1, where only the edges in  $\Lambda \setminus S$  are shown and the arrows indicate assignment of some vertices  $A_n$  and  $B_n$ , with  $|n|$  small, via  $s = s^1$ .

Now, PDSs whose induced components are parallel, horizontal, 1-cubes can only be images of  $\{0, 1\}$ -sequences through the just introduced one-to-one correspondence, for otherwise a path of length 3 would be found as an induced component of such a PDS, as in the bottom of Figure 1, a contradiction. In particular, we conclude that there are no less PDSs in  $\Lambda$  than doubly infinite binary sequences, whose cardinality surpasses  $\aleph_0$ .  $\square$

**Corollary 2** *There is no algorithmic characterization for PDSs in  $\Lambda$ .*

*Proof.* Because of the uncountability of total perfect codes in  $\Lambda$  found in Theorem 1, it is clear that there cannot be such algorithmic characterization.  $\square$

Given a PDS  $S$  in  $\Lambda$ , the graph  $\Lambda \setminus S$  has chordless cycles delimiting rectangles of areas at least 4, that we call *rooms*, and maximal connected unions of 4-cycles arranged either horizontally or vertically into rectangles, that we call *ladders*, a possible case of which is a single 4-cycle bordered by rooms. The totality of ordered pairs formed by the horizontal and vertical dimensions, (widths and heights), of the rectangles spanned by these rooms and ladders can be presented in an array of integer pairs that we call the *PDS-array* associated to  $S$ . For example, the PDS partially depicted in the upper part of Figure 1 has a PDS-array correspondingly containing the following disposition of ordered pairs of (one-digit) integers (with deleted parentheses and commas):

$$\begin{array}{cccccccccccccccc} \dots & 12 & 32 & 12 & 32 & 21 & 32 & 12 & 32 & 12 & 32 & 21 & 32 & 21 & 32 & \dots \\ \dots & 32 & 12 & 32 & 12 & 32 & 21 & 32 & 12 & 32 & 12 & 32 & 21 & 32 & 21 & \dots \\ \dots & 12 & 32 & 12 & 32 & 12 & 32 & 21 & 32 & 12 & 32 & 12 & 32 & 21 & 32 & \dots \\ \dots & 32 & 12 & 32 & 12 & 32 & 32 & 21 & 32 & 12 & 32 & 12 & 32 & 21 & 32 & \dots \\ \dots & 12 & 32 & 12 & 32 & 12 & 12 & 12 & 32 & 21 & 32 & 12 & 32 & 12 & 32 & \dots \end{array}$$

with the pairs  $32 = (3, 2)$  in the second and third rows representing the rooms containing the vertices  $A_i, B_i$  in the figure and its destination vertices  $s(A_i), s(B_i)$ ,

respectively, for  $i = -2, \dots, 4$ . The pairs in a PDS-array giving the dimensions of a room, (ladder), are called *room pairs*, (*ladder pairs*).

Let TPC stand for total perfect code. Let  $\Psi$  denote the correspondence in Theorem 1 that assigns to each doubly infinite binary sequence  $(\dots, a_i, \dots, a_0, \dots, a_i, \dots)$  a *parallel* TPC (PTPC) in  $\Lambda$ , meaning that its induced 1-cubes are pairwise parallel.

**Corollary 3** *The family of TPCs  $S$  in  $\Lambda$  having only ladder pairs of the form  $(2, 1) = 21$  is in one-to-one correspondence with the set of doubly infinite  $\{0, 1\}$ -sequences.*

*Proof.* Consider the translated lattice graph  $\Lambda' = \Lambda + (\frac{1}{2}, \frac{1}{2})$ . Given a doubly infinite binary sequence  $A = (\dots, a_i, \dots, a_0, \dots, a_i, \dots)$ , we construct a TPC  $\Psi'(A)$  in  $\Lambda'$  as in the statement of the corollary by selecting its component vertices (in  $\Lambda'$ , instead of  $\Lambda$ ) as the barycenters of the unit-area squares delimiting the 4-cycles of  $\Lambda \setminus \Psi(A)$ . Then, by taking  $\Psi''(A) = \Psi'(A) - (\frac{1}{2}, \frac{1}{2})$ , we get a one-one correspondence as required.  $\square$

The PDS-array partially presented above in relation to the example of Figure 1, for a PTPC  $\Psi(\dots, 0, 0, 1, 0, 0, 1, 1, \dots)$ , has a counterpart due to the argument of Corollary 3, which is the PDS-array for the TPC

$$\Psi''(\dots, 0, 0, 1, 0, 0, 1, 1, \dots),$$

correspondingly representable as follows:

$$\begin{array}{cccccccccccccccccccc} \dots & 23 & 21 & 23 & 21 & 32 & 21 & 23 & 21 & 23 & 21 & 32 & 21 & 32 & 21 & \dots \\ \dots & 21 & 23 & 21 & 23 & 21 & 32 & 21 & 23 & 21 & 23 & 21 & 32 & 21 & 32 & \dots \\ \dots & 23 & 21 & 23 & 21 & 23 & 21 & 32 & 21 & 23 & 21 & 23 & 21 & 32 & 21 & \dots \\ \dots & 21 & 23 & 21 & 23 & 21 & 21 & 21 & 32 & 21 & 23 & 21 & 23 & 21 & 32 & \dots \\ \dots & 23 & 21 & 23 & 21 & 23 & 23 & 23 & 21 & 32 & 21 & 23 & 21 & 23 & 21 & \dots \end{array}$$

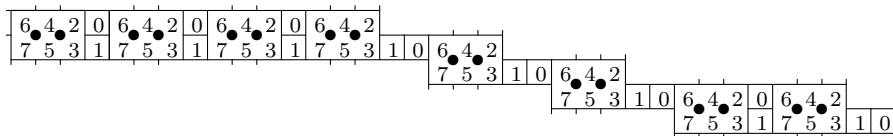
obtained from the previously given PDS-array by subtracting 1 from each one of the two component integers of each room pair and adding 1 to each one of the two component integers of each ladder pair.

We may say that the relation between  $\Psi(A)$  and  $\Psi'(A)$  is one of *room-ladder duality*. This applies, more generally, to all PDSs  $S$  in  $\Lambda$  whose complementary graphs  $\Lambda \setminus S$  in  $\Lambda$  have PDS-arrays with room pairs  $(r, s)$  satisfying only  $\min\{r, s\} = 2$ . This extends to PDSs in quotient graphs in  $\Lambda$  of the form  $C_m \times C_n$ , where  $\min\{m, n\} \geq 3$ .

Theorem 1 may have been expressed for PDSs whose induced components are parallel, vertical, 1-cubes. Corollary 3 may have been expressed for TPCs having only ladder pairs of the form  $(1, 2) = 12$ .

### 3 PTPCs in cycle products

By restricting  $\Psi$  to periodic doubly infinite binary sequences, we find the following result. A binary  $n$ -tuple has *weight*  $k$  if and only if it has exactly  $k$  unit entries.



**Theorem 4** *A periodic doubly infinite binary sequence with period  $B = (b_1, b_2, \dots, b_n)$  of weight  $k$  is sent by  $\Psi$  into a PTPC  $\Psi(B)$  in  $\Lambda$  that covers a PTPC  $\Phi(B)$  in the Cartesian product  $C_p \times C_p$ , where  $p = 4n$  if  $k$  is even, and  $p = 8n$  if  $k$  is odd. This establishes a one-one correspondence  $\Phi$  from the irreducible periodic doubly infinite binary sequences onto the irreducible horizontal PTPCs in Cartesian products of two cycles.*

In the PDS-array associated to one such  $\Psi(B)$ , there are only two types of horizontally contiguous pairs of entries (which are integer pairs) formed by a leftmost room pair and a rightmost ladder pair, namely:  $(32, 12)$  and  $(32, 21)$ . For example, Figure 2 shows the first stage of the procedure in the proof of Theorem 1 applied to the irreducible period  $B = 00011101$ , producing concretely the *fundamental tile*  $\mathcal{T}(B)$  associated to  $B$ , before extending it periodically to its (upper-)left and to its (lower-)right sides and applying subsequently the transformation  $s$  of Theorem 1 and its powers in order to exhibit  $\Psi(B)$ . Observe that each null entry in this  $B$  has associated a pair  $(32, 12)$  and each non-null entry in it has associated a (descending) pair  $(32, 21)$ .

The unit-area squares determined by the 4-cycles of  $\Lambda$  in the Euclidean plane are labeled for convenience as shown in Figure 2, which establishes a fixed labeling of the realizations of the pairs  $(32, 12)$  and  $(32, 21)$  in  $\Psi(B)$ . By extending the period  $B$  to left and right and applying  $s$  and its powers, a larger picture of this labeling representing  $\Psi(B)$  can be seen as a  $32 \times 32$  array  $M = M(00011101)$  produced by these labels of unit-area squares, whose first two rows form the sub-array  $M_1 = M_1(00011101) =$

6 4 2 0 6 4 2 0 6 4 2 0 6 4 2 7 5 3 1 0 6 4 2 7 5 3 1 7 5 3 1 0  
7 5 3 1 7 5 3 1 7 5 3 1 7 5 3 1 0 6 4 2 7 5 3 1 0 6 4 2 0 6 4 2

from which the whole array can be obtained by means of the following induction step, where  $j = 0, \dots, 15$ : Let  $M_j$  be the sub-array of  $M$  formed by the  $(2j+1)$ -th and  $(2j+2)$ -th rows of  $M$ . If  $M_j = (X, Y)$ , where  $Y$  is the rightmost  $2 \times 2$  sub-array

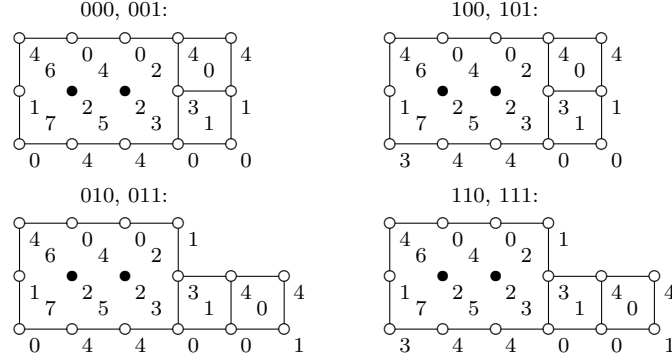


Figure 3: Labelled room-label pairs for middle entries of binary triples

of  $M_j$ , then  $M_{j+1} = (Y, X)$ . This induction step is produced by the transformation  $s$  and what follows.

The union of the  $32 \times 32 = 1024$  4-cycle-delimiting unit squares whose labels are arranged precisely as in  $M(B)$  form a square  $N(B)$  of side length 32 in the Euclidean plane. By identifying the top and bottom sides of  $N(B)$  as well as its left and right sides, a (flat) torus  $\mathcal{S}$  is obtained, (flat torus in the sense of [4]). In  $\mathcal{S}$ , the projections of the original vertices and edges of  $\Lambda$  form the Cartesian product  $C_p \times C_p$  ( $p = 32$ ). In this  $C_p \times C_p$ , the PTPC  $S$  in  $\Lambda$  determined by the period  $B = 00011101$  projects onto a PTPC  $\bar{S}$  in  $C_p \times C_p$ , as required in the statement of the theorem. Also,  $N(B)$  can be furnished as a *cutout* of  $\mathcal{S}$  in which  $S$  or  $\bar{S}$  can be visualized, as is done down below in Figures 4 and 5 for the first two even- and odd-weight cases of periods  $B$  in their listings as indicated above, respectively.

Given a PDS  $S$  in  $\Lambda$ , a labeling  $f_S$  of  $\Lambda$  with symbols in  $\{0, 1, 2, 3, 4\}$  is defined as follows: let 2 label each  $v \in S$ ; for each vertex  $v$  of  $\Lambda \setminus S$ , let 0,1,3,4 label  $v$  if  $v - (0, 1), v - (1, 0), v + (1, 0), v + (0, 1)$  belongs respectively to  $S$ .

The exemplified period  $B = 00011101$  contains all eight cases of possible binary triples. The vertex labels of  $f_S$  associated to the room-ladder pairs in the image of the middle entries of such triples through  $\Psi$  are as shown in Figure 3, (where also the unit-area squares determined by the 4-cycles of  $\Lambda$  are labeled in their centers as indicated above).

In general, a fundamental tile  $\mathcal{T}(B)$  is determined, for any period  $B$  of a periodic doubly infinite binary sequence by replacing each entry  $b_i = 0$  of  $B$  by a sub-tile  $\tau_0$  as in the two top cases of Figure 3, formed by a room-ladder pair with PDS-sub-array  $(32, 12)$ , and by replacing each entry  $b_i = 1$  of  $B$  by a sub-tile  $\tau_1$  as in the two bottom cases of Figure 3, formed by a room-ladder pair with PDS-sub-array  $(32, 21)$ . If  $b_i = 0$ , then the unit-area squares with labels 0 and 1 in  $\tau_0$  are adjacent to their right to unit-area squares with respective labels 7 and 6, belonging to a sub-tile of either type. if  $b_i = 1$ , then the unit-area square with label 0 is adjacent to its right to a unit-area square with label 7, that is at the upper-left corner of another sub-tile. This composed periodically (for a fixed period  $B$ ) and translated by the powers of  $s$  yields  $\Psi(B)$ .

Given a period  $B$  of a periodic doubly infinite binary sequence, let  $B_1$  be the subsequence of  $B$  whose last entry is the first, or leftmost, unit entry of  $B$ . Induc-

tively for  $1 < i \leq k$ , let  $B_i$  be the subsequence of  $B \setminus (\cup_{j=1}^{i-1} B_j)$  whose last entry is the  $i$ -th unit entry of  $B$ , where  $B \setminus (\cup_{j=1}^{i-1} B_j)$  is the subsequence of  $B$  obtained by deleting the successive concatenation of  $B_1, B_2, \dots, B_{i-1}$ . The sequence  $\xi(B_1)$  of labels of unit-area squares in the first, or top, row of  $\mathcal{T}$  is obtained by successively replacing each null entry of  $B_1$  by a subsequence 6420, and the final unit entry of  $B_1$  by a subsequence 642. There is an accompaniment of this  $\xi(B_1)$  by a sequence  $\eta(B_1)$  in the second row of such labels in  $\mathcal{T}(B)$ : below each subsequence 6420 in  $\xi(B_1)$ , corresponds a subsequence 7531; below the final subsequence 642 of  $\xi(B_1)$  corresponds a subsequence 75310, extended two extra positions to the right of the final entry of  $\xi(B_1)$ . From the subsequent position to the right of this final entry of  $\xi(B_1)$ ,  $\mathcal{T}$  contains  $\xi(B_2)$ , and below it,  $\eta(B_2)$ , and so on, down to  $\xi(B_k)$  and  $\eta(B_k)$ .

For  $B = 00011101$ , the first row of  $M_1(B)$  is formed by the concatenation of the first, third and fifth rows of  $\mathcal{B}$ , namely  $\xi(B_1) = \xi(0001) = (6420)^3 642$ ,  $\eta(B_2)\xi(B_3) = \eta(1)\xi(1) = 75310642$  and  $\eta(B_4) = \eta(01) = (7531)^2 0$ , respectively; the second row of  $M_1(B)$  is formed by the concatenation of the second and the fourth rows of  $\mathcal{B}$ , namely  $\eta(B_1)\xi(B_2) = \eta(0001)\xi(1) = (7531)^4 0642$  and  $\eta(B_3)\xi(B_4) = \eta(1)\xi(01) = 7531(0642)^2$ , respectively.

Similarly for any other period  $B$  of even weight  $k$ : the first (second) row of  $M_1(B)$  is the concatenation of the odd (even) rows of  $\mathcal{T}(B)$  in their increasing order, which is then repeated periodically in  $\Lambda$  by way of horizontal concatenations. Observe that the rows of  $\mathcal{T}(B)$  have successively the following label sequences, or concatenations of label sequences:

$$\xi(B_1), \eta(B_1)\xi(B_2), \dots, \eta(B_i)\xi(B_{i+1}), \dots, \eta(B_{k-1})\xi(B_k), \eta(B_k),$$

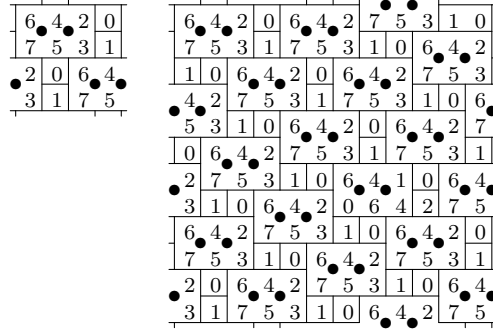
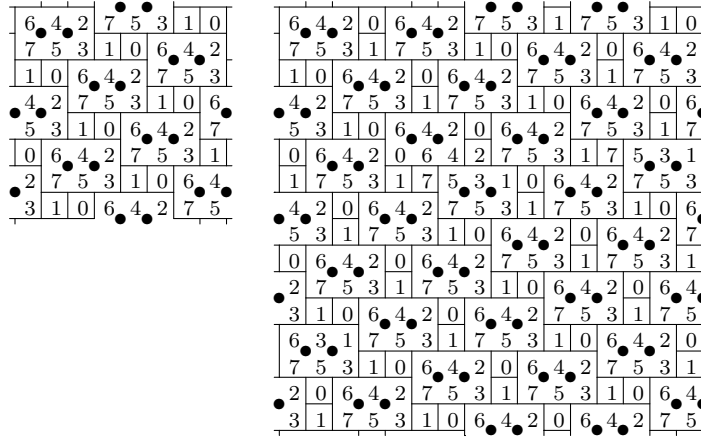
from which we must select the concatenation of the odd- (even-) positioned member label subsequences as the first (second) row of  $M_1(B)$ , whose total length is then seen to be  $4k$ ,  $(4k)$ .

For each period  $B$  of odd weight  $k$ , the first (second) row of  $M_1(B)$  is the concatenation of the odd (even) rows of  $\mathcal{T}(B)$  followed by the concatenation of the even (odd) rows of  $\mathcal{T}(B)$ , in their increasing order in both cases.

The total length of the concatenations in either the first of the second row is  $p = 4n$  if the weight  $k$  of  $B$  is even and is  $p = 8n$  if  $k$  is odd. This implies the statement of the theorem.  $\square$

**Corollary 5** *A PTPC in a Cartesian product  $C_m \times C_n$  of two cycles  $C_m$  and  $C_n$  exists if and only if  $m$  and  $n$  are multiples of 4.*

*Proof.* Let  $B$  be a fixed period  $B$  of a periodic doubly infinite binary sequence. By taking the union of several contiguous copies of  $N(B)$  conforming a square or rectangle  $N'$  in the Euclidean plane, or just  $N' = N(B)$ , and identifying the top and bottom sides of  $N'$  as well as the left and right sides of  $N'$ , it is seen that a toroidal graph of the form  $C_m \times C_n$  is obtained that contains a PTPC. Because of Theorems 1 and 4, both  $m$  and  $n$  must be multiples of 4. Moreover, no other sources of PTPCs in Cartesian product of cycles exist.  $\square$

Figure 4: First two even-weight cases:  $M(0)$  and  $M(011)$ Figure 5: First two odd-weight cases:  $M(1)$  and  $M(01)$ 

Each Cartesian product  $C_m \times C_n$  of cycles  $C_m$  and  $C_n$  of lengths  $m$  and  $n$  larger than 2, respectively, is the target of a *canonical projection* graph map  $\rho$  from  $\Lambda$  onto  $C_m \times C_n$  such that  $\rho(i, j) = (i \bmod m, j \bmod n)$ , where  $i \bmod m$  and  $j \bmod n$  are the remainders of dividing  $i$  and  $j$  respectively by  $m$  and  $n$ . Clearly,  $\rho$  is surjective graph homomorphism.

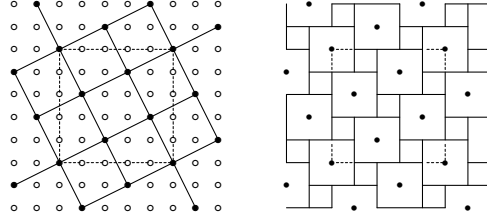
**Corollary 6** *A TPC in a Cartesian product  $C_m \times C_n$  producing only ladder pairs of the form 21 in the inverse-image TPC in  $\Lambda$  via  $\rho$  exists if and only if  $m$  and  $n$  are multiples of 4.*

*Proof.* The statement of the corollary arises by combining Corollary 3 and Theorem 4. □

#### 4 $d$ -Perfect code partitions of $\Lambda$ and $C_m \times C_n$

In contrast with the uncountability of Theorem 1, there is just one 1-perfect code  $S_0$  in  $\Lambda$ , up to symmetry, which can be taken as the sublattice of  $\Lambda$  generated by  $\{(1, 2), (2, -1)\}$ . (A generalization of this fact is given in Section 8 for integer




 Figure 6: 1-Perfect code in  $\Lambda$  and a cutout for  $C_5 \times C_5$ 

lattices in  $\mathbf{R}^r$ ,  $r \geq 2$ ). Figure 6 partially depicts  $S_0$  and its complementary graph in  $\Lambda$ . Moreover,  $S_0$  does not restrict to a 1-perfect code in any rectangular grid graph  $\Gamma_{m,n}$  with  $m$  or  $n$  larger than 4. The center  $4 \times 4$  grid graph  $\Gamma_{4,4}$  in the interior of the dotted line in Figure 6 depicts the only existing 1-perfect code in a  $\Gamma_{m,n}$  with  $\min\{m, n\} > 2$ , up to symmetry, [9]. (It is not difficult to visualize 1-perfect codes in  $\Gamma_{m,n}$  if  $m = 1$  or  $2$ , in the latter case with  $n$  odd).

$V(\Lambda)$  admits a partition into five copies of  $S_0$ . Now, the total number of perfect codes isomorphic to  $S_0$  in  $\Lambda$  is ten, of which five are tilted as in Figure 6 and five are tilted in the other way, composing two *enantiomorphic* presentations of  $S_0$ , (mirror images of each other). Thus, there are two possible partitions of  $\Lambda$  into copies of  $S_0$ , or of its enantiomorphic code in  $\Lambda$ .

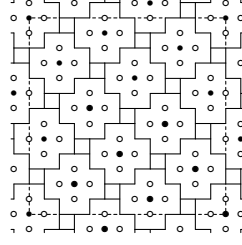
Moreover, there are 1-perfect codes in toroidal graphs, specifically Cartesian products  $C_{5k} \times C_{5\ell}$ , for  $0 < k, \ell \in \mathbf{Z}$ , obtained from  $S_0$  and having cardinality  $5k\ell$ . (The existence of such a code would follow from Theorem 2.5 of [9], but look at the remark after Theorem 11 in Section 6.)

An example of such 1-perfect code in  $C_5 \times C_5$  can be visualized in Figure 6, where the dotted lines delineate the boundary of a cutout of the (flat) torus involved; the left side of the figure represents the minimum-distance graph of  $S_0$ , which is the restriction of the power graph  $(\Lambda)^3$  to  $S_0$ ; the right side represents the complementary graph of  $S_0$  in  $\Lambda$ . No other 1-perfect codes in Cartesian products of two cycles exist.

**Theorem 7** *There exists a toroidal graph  $C_m \times C_n$  having a 1-perfect code partition  $\mathcal{S}_0 = \{S_0^0 = S_0, S_0^1, \dots, S_0^4\}$  if and only if  $m$  and  $n$  are multiples of 5. Each component code  $S_0^i$  of  $\mathcal{S}_0$ , which is a translate of the sublattice  $S_0$ , has cardinality  $mn/5$  and cannot be obtained by side identifications from 1-perfect codes in any rectangular grid graph.*

Theorem 7 is a particular case of the following result. Recall from [3] that for  $d \geq 1$ , a  $d$ -perfect code in a regular graph  $G$  is a vertex subset  $S$  such that every vertex  $v$  in  $G \setminus S$  is at distance  $\leq d$  from just one vertex  $w(v)$  of  $S$ . Notice however that no  $G \setminus S$  is 3-regular, for any  $d$ -perfect code  $S$  in a 4-regular graph  $G$ , when  $d > 1$ , contrary to the observation previous to Theorem 1. Figure 7 illustrates this point.

A  $d$ -perfect code  $S$  in  $\Lambda$  can be found easily, following inductively a construction whose first two steps are illustrated in Figures 6 and 7, for  $d = 1, 2$  respectively. Given such an  $S$ , the vertices of the  $d$ -neighborhood  $N_d(v)$  of any vertex  $v$  of  $S$  are labeled as follows: the top element of  $N(v)$  gets label 1; the vertices of the longest

Figure 7: 2-Perfect code in  $\Lambda$  and a cutout for  $C_{13} \times C_{13}$ 

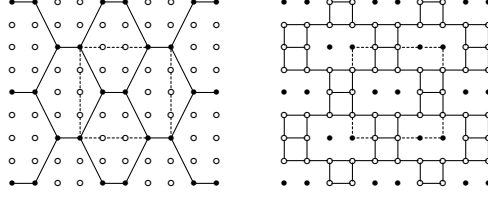
horizontal path of  $N(v)$ , that is the  $(d+1)$ -th horizontal path, of length  $2d+1$ , get the subsequent integer labels from left to right:  $2, 3, \dots, 2d+2$ ; the bottom vertex of  $N(v)$  gets label  $2d+3$ ; if there are still horizontal paths with unlabeled vertices in  $N(v)$ , then the  $d$ -th and  $2d$ -th horizontal paths of  $N(v)$  receive the subsequent integer labels increasingly from left to right; and so on, if necessary, with the  $(d-1)$ -th and  $(2d-1)$ -th horizontal paths, etc.

In other words, by denoting the rows of vertices of  $N(v)$  from top to bottom successively as row 1, row 2,  $\dots$ , row  $(2d+1)$ , and by considering this row order cyclically mod  $2d+1$ , we label with  $1, 2, \dots, 2d^2+2d+1 = q$  subsequently from left to right the vertices in the rows  $1, 1+d, 1+2d, \dots, 1+(2d)d = d+2 \pmod{2d+1}$ , in that order. For Figures 6 and 7, this looks respective as follows:

$$\begin{array}{ccccccc}
 & & & & 1 & & \\
 & & & & 8 & 9 & a \\
 1 & & & & 2 & 3 & 4 & 5 & 6 \\
 2 & 3 & 4 & & & & & & \\
 & & & & 5 & & & & b & c & d \\
 & & & & & & & & & & 7
 \end{array}$$

where hexadecimal notation is used. (This coincides with a case of [12], leading to the graph  $\mathcal{Q}_d$  in Corollary 9 below. Compare also with [1, 4]). The advantage of this labeling is that it can be extended to all  $d$ -neighborhoods of vertices of  $S$  so that in each row the labels from 1 to  $q = 2d^2 + 2d + 1$  appear subsequently and contiguously from left to right, which in the cases of Figures 6 and 7 makes that the first row of the depicted cutout of  $C_q \times C_q$  receives the following labels from left to right: 3 4 5 1 2 3 and 4 5 6 7 8 9 a b c d 1 2 3 4 respectively, and so on for the remaining rows of the cutout, comprising all the numbers in the range  $1, 2, \dots, 2d(d+1)$  in increasing order mod  $q$  from left to right, from certain vertex on, and then extended periodically for the vertices of each horizontal path in  $\Lambda$ . Observe that the disposition of these labels yields a  $q \times q$  Latin square and that the vertices having any fixed label constitute a translate of the sublattice of  $\Lambda$  generated by  $\{(d, d+1), (d+1, -d)\}$ .

**Theorem 8** *There exists a toroidal graph  $C_m \times C_n$  having a  $d$ -perfect code partition  $\mathcal{S}_{d-1} = \{S_{d-1}^0 = S_{d-1}, S_{d-1}^1, \dots, S_{d-1}^{q-1}\}$ , where  $q = 2d^2 + 2d + 1$ , if and only if  $m$  and  $n$  are multiples of  $q$ . Each of the component codes  $S_{d-1}^i$  of  $\mathcal{S}_{d-1}$  has cardinality  $mn/q$  and cannot be obtained by side identifications from 1-perfect codes in any rectangular grid graph.*


 Figure 8: Total perfect code in  $\Lambda$  and a cutout for  $C_4 \times C_4$ 

*Proof.* Since a cutout square  $P_q \times P_q$  of  $C_q \times C_q$  projects onto  $q^2$  different vertices of  $C_q \times C_q$  and since any  $d$ -neighborhood of a vertex of  $\Lambda$  contains  $q$  vertices, then the projected code from  $S$  in  $C_q \times C_q$  contains  $q$  vertices. The statement of the theorem follows by forming larger cutouts which are rectangular arrangements obtained by continuation of copies of the original cutout.  $\square$

**Corollary 9** *Identification of vertices in  $\Lambda$  with each common label  $i = 1, 2, \dots, q = 2d^2 + 2d + 1$  yields the quotient graph  $\mathcal{Q}_d$  of its partition into  $q$   $d$ -perfect codes. Moreover,  $\mathcal{Q}_d$  is a 4-regular bipartite graph, namely the undirected Cayley graph of the cyclic group  $Z_q$  under the generator set  $\{1, 2d^2\}$ .*

*Proof.* What is the difference mod  $q$  between the label of any vertex  $w$  of  $\Lambda$  and the label of the vertex immediately below  $w$ ? We answer this on the central, longest, vertical path, or column of vertices, of  $N(v)$ . Observe that the labels in this path start in its top vertex with label 1 and continue with labels that increase mod  $q$  in subsequent increments of value  $2d^2$ . This is due to the fact that by starting with the vertex labeled 1 and descending in this column cyclically mod  $2d + 1$  by jumping  $d$  rows in each of  $2d + 1$  instances, we cover subsequently the central position in the rows  $1, d + 1, 2d + 1, d, 2d, d - 1, 2d - 1, \dots, 2, 2 + d$  and again 1. By finishing this process in label 2, two steps before returning to label 1, we obtain the sequence of  $2d - 1$  subsequent label differences  $d + 2, d + 2, d + 1, \dots, d + 2, d + 1$ , which starts with  $d + 1$  twice and then alternating  $d + 1$  with  $d + 2$ , amounting to  $d$  times  $d + 1$  plus  $d - 1$  times  $d$ . We conclude that  $\mathcal{Q}_d$  is the 4-regular bipartite graph whose vertex set is the cyclic group  $Z_q = \{1, 2, \dots, q - 1, q = 0\}$ , with vertices  $i$  and  $j$  adjacent if and only if  $i - j \in \{1, -1, 2d^2, -2d^2\}$ . Thus,  $\mathcal{Q}_d$  is the claimed Cayley graph.  $\square$

Of course, Corollary 9 holds with  $\Lambda$  replaced by any  $C_m \times C_n$  as in Theorem 8. Continuing the remark that ends the second paragraph of this section, we note that there are only two possible partitions of  $\Lambda$  into copies of a  $d$ -perfect code of  $\Lambda$ , corresponding to the two enantiomorphic presentations of such a code. In the second such code, the labeling of the vertices of an  $N(v)$  ascends on each row from right to left, instead of being from left to right.

## 5 Total perfect code partitions of $\Lambda$

Among the PTPCs in  $\Lambda$  arising from Theorem 1, there is only one, call it  $S_2$ , such that  $\Lambda$  admits a partition into copies of  $S_2$  that can be projected onto a partition

of  $C_4 \times C_4$ , based on the PTPC corresponding to the null  $\{0, 1\}$ -sequence, and due to Corollary 5. The total number of copies of such PTPC  $S_2$  existing in  $\Lambda$  is 16, of which eight have just horizontal (vertical) induced edges, yielding four possible partitions of  $\Lambda$  into copies of  $S_2$ .

From Corollary 5, it can be seen that there are PTPCs in toroidal graphs  $C_{4k} \times C_{4\ell}$ , for  $0 < k, \ell \in \mathbf{Z}$ , obtained from  $S_2$  by means of identifications in  $\Lambda$  and having cardinality  $4k\ell$ . An example of such PTPC in  $C_4 \times C_4$  can be visualized in Figure 8, where the dotted lines delineate the boundary of a cutout from which the (flat) torus involved can be obtained; the left side of the figure represents part of the restriction of  $(\Lambda)^3$  to  $S_2$ ; the right side represents the complementary graph of  $S_2$  in  $\Lambda$ .

**Theorem 10** *Let  $1 < m, n \in \mathbf{Z}$ . There exists a toroidal graph  $C_m \times C_n$  having a PTPC partition  $\mathcal{S}_2 = \{S_2^0 = S_2, S_2^1, S_2^2, S_2^3\}$  if and only if  $m$  and  $n$  are multiples of 4. Each component PTPC  $S_2^i$  in  $\mathcal{S}_2$  has cardinality  $mn/4$  and cannot be obtained by side identifications from PTPCs in any rectangular grid graph.*  $\square$

## 6 A Penrose-tiling-like total perfect code

In [7], it was shown that an  $m \times n$  grid graph  $\Gamma_{m,n}$  with  $\min\{m, n\} > 1$  contains a TPC if and only if  $m \equiv 0 \pmod{2}$  and  $n \equiv -3, -1$  or  $1 \pmod{m+1}$ .

In [5], this was used to show that there is only one TPC  $S_1$  in  $\Lambda$  that restricts to TPCs in rectangular grid graphs  $\Gamma_{m,n}$ , where  $m$  and  $n$  are integers  $> 2$ . Moreover, the complement  $\Lambda \setminus S_1$  yields an aperiodic tiling of the plane (like the Penrose tiling, [10]) whose automorphism group coincides with the group  $D_8$  of the square  $[-\frac{1}{2}, \frac{1}{2}] \times [-\frac{1}{2}, \frac{1}{2}]$ .

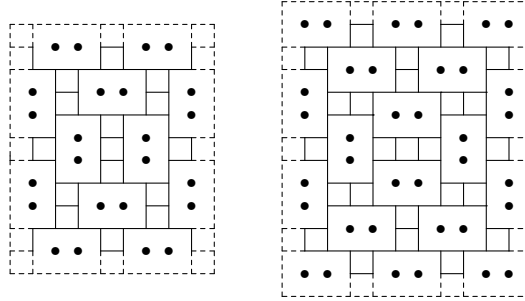
Again, this result is in contrast with the uncountability of TPCs shown in Theorem 1.

It is impossible to partition  $\Lambda$  into copies of the graph  $S_1$ , nor there are quotient toroidal graphs in  $\Lambda$  containing a TPC obtained by projecting  $S_1$ , because of the presence of a unique central ladder of area 3 in the complementary graph of  $S_1$  in  $\Lambda$ , while all the other ladders have area 2. See Figure 9, where two concentric stages in the construction of  $S_1$  and of  $\Lambda \setminus S_1$  are shown. Observe that the leftmost stage must be rotated 90 degrees in order for its immersion into the second stage to be visualized, with intermittent lines added for ease of comprehension of the immersion (and in accordance with the definition of PDS-arrays of graphs  $\Gamma_{m,n}$  in [5]).

## 7 PDSs in other toroidal grid graphs

Denote by  $C_2$  the multigraph composed by two vertices and two parallel edges between them. We have the following complementary results.

**Corollary 11** *A PTPC in a  $C_2 \times C_n$  exists if and only if  $n$  is a multiple of 6.*


 Figure 9: Two stages in the construction of  $S_1$  and  $\Lambda \setminus S_1$ 

*Proof.* Let  $C_2 \times C_{6k}$  be represented in a (flat) torus obtained from the immersion of the rectangular sub-grid of  $\Lambda$  that has vertex set  $\{(i, j); 0 \leq i \leq 2; 0 \leq j \leq 6k\}$  into the Euclidean plane, by means of vertex identifications  $(i, 0) \equiv (i, 6k)$ , for  $0 \leq i \leq 2$ , and  $(0, j) \equiv (2, j)$ , for  $0 \leq j \leq 6k$ , and corresponding edge identifications. Then, a PTPC in  $C_2 \times C_{6k}$  is given by the projection of the vertices  $(0, 1 + 6i), (0, 2 + 6i), (1, 4 + 6i), (1, 5 + 6i)$ , where  $0 \leq i < k$ .  $\square$

**Theorem 12** *There exists a toroidal graph  $C_2 \times C_n$  having a 1-perfect code partition  $\mathcal{S}_0$  if and only if  $n$  is divisible by 4. In this case,  $\mathcal{S}_0$  contains four 1-perfect codes, and the component codes cannot be obtained by side identifications from 1-perfect codes in any rectangular grid graph.*

*Proof.* Let  $C_2 \times C_{4k}$  be represented in a (flat) torus obtained from the immersion of the rectangular sub-grid in  $\Lambda$  possessing vertex set  $\{(i, j); 0 \leq i \leq 2; 0 \leq j \leq 4k\}$  into the Euclidean plane by means of the vertex identifications  $(i, 0) \equiv (i, 4k)$ , for  $0 \leq i \leq 2$ , and  $(0, j) \equiv (2, j)$ , for  $0 \leq j \leq 4k$ , accompanied by the corresponding edge identifications. Then, one of the 1-perfect codes in  $\mathcal{S}_0$  is given by the projection of the vertices  $(1, 0 + 4i), (0, 2 + 4i)$ , where  $0 \leq i < k$ . (An example of this for  $k = 1$  is given on the left side of Figure 10, commented in a remark below). The other three 1-perfect codes here are obtained by translation along the vectors  $(1, 0), (0, 1), (1, 1)$ .  $\square$

Theorem 2.5 of [9] announces correctly the existence of the code  $S_0$  mentioned in Section 3 above. However, it also claims the existence of a 1-perfect code in  $C_4 \times C_6$ , which is incorrect. The right side of Figure 10 serves to get a counterexample: we can select successively vertices  $u, v, w$  as members of a candidate 1-perfect code in  $C_4 \times C_6$ , as depicted in the figure, (where diagonals join the dominated vertices of each of  $u, v, w$ ; notice that after selecting vertex  $u$ , the only dominating vertex for  $s$ , up to symmetry, is  $v$ , and then the only dominating vertex for  $t$  is  $w$ ). But then vertex  $x$  cannot form part of any such 1-perfect code, nor can be dominated by any vertex of it.

The left side of Figure 7 shows a detachment of  $C_2 \times C_4$  showing a 1-perfect code  $\{u, v\}$ , as correctly cited in the mentioned theorem. Generally, diagonals joining dominated vertices would form square rhombuses, but in this case, the rhombus

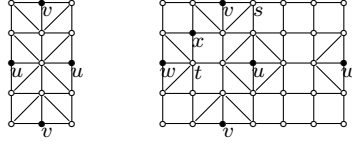


Figure 10: Example and counterexample for Theorem 2.5 of [9]

around  $u$  is a degenerate one, because two opposite vertices of the rhombus are identified.

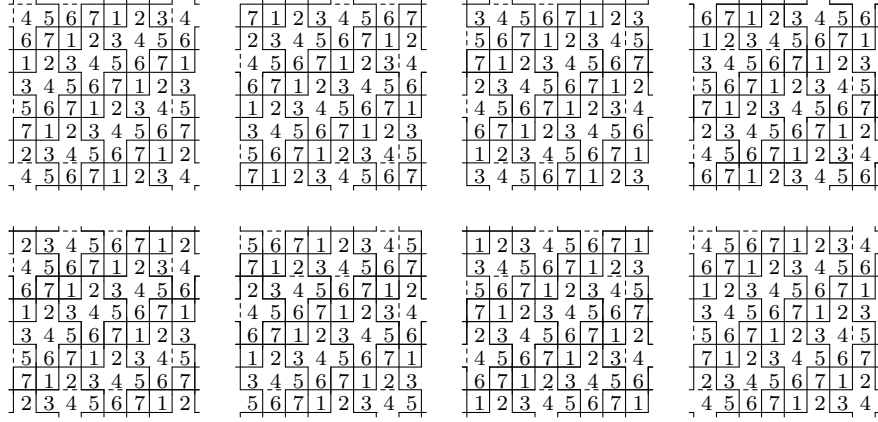
## 8 Case of integer lattice graphs of $\mathbf{R}^r$ , $r \geq 2$

Let  $1 < r \in \mathbf{Z}$ . In this section, we replace  $\Lambda = \Lambda^2$  by the integer lattice graph  $\Lambda^r$  of  $\mathbf{R}^r$ . We extend facts and results in Section 4 to  $\Lambda^r$  as follows, noticing that this can only be done for  $d = 1$  if  $r > 1$ , in the notation of Section 4.

**Theorem 13** *There exists a linear 1-perfect code  $S_0$  in  $\Lambda^r$ . Moreover,  $S_0$  can be taken as the sublattice of  $\Lambda^r$  generated by the vectors  $(1, r, 0, \dots, 0)$ ,  $(2, -1, 0, \dots, 0)$ ,  $(3, 0, -1, 0, \dots, 0)$ ,  $\dots$ ,  $(r, 0, \dots, 0, -1)$ . Furthermore,  $S_0$  does not restrict to a 1-perfect code in any  $r$ -dimensional parallelepiped grid graph  $\Gamma_{m_1, m_2, \dots, m_r}$  with at least one of  $m_1, m_2, \dots, m_r$  larger than 4.*

*Proof.* We consider the vertices of  $\Lambda^r$  as centers of  $r$ -dimensional cubes with unit-length edges that are parallel to the coordinate axes of  $r$ -space. The collection of all such cubes forms a tessellation of  $\mathbf{R}^r$  which can be interpreted as a Voronoi diagram, [4]. Each cube in such a tessellation receives a label in the range  $1, 2, \dots, 2r + 1$  according to the following rule, which extends the case  $d = 1$  of the argument previous to Theorem 8 and Corollary 9, above. Let  $r + 1$  label the null vertex of  $\Lambda^r$ ; let  $r + 1 + i\delta$  label the vertex having all coordinates null but for the  $i$ -th coordinate, which equals  $\delta = \pm 1$ . Extend this labeling initialization by making the difference  $\ell(w) - \ell(v)$  of the labels  $\ell(v)$  and  $\ell(w)$  of two contiguous vertices  $v = (v_1, v_2, \dots, v_r)$  and  $w = (w_1, w_2, \dots, w_r)$  equal to  $\ell(w) - \ell(v) = i$ , where  $w_j = v_j$  if  $j \neq i$  and  $w_i = v_i + 1$ . The vertices of  $\Lambda$  having any fixed label  $1, \dots, 2r + 1$  constitute a translate of the sublattice generated by the vectors cited in the statement. The resulting labeling of the vertices of  $\Lambda^r$  is as claimed. The second assertion of the statement arises from an observation in the first paragraph of Section 4, after our citing Figure 6.  $\square$

Figure 11 illustrates, for  $r = 3$ , the labeling indicated in Theorem 13 by means of a partial representation of the mentioned Voronoi-diagram tessellation, which in this case is 3-dimensional. The figure only shows eight partially horizontal levels of such tessellation, where (a) each edge represents a 4-cycle face looked upon from above; (b) each vertex represents the intersection edge of two such faces; (c) the first (upper-left) and eighth (lower-right) levels coincide. Only faces of outlines of 3-dimensional crosses with central cube labeled 4 and remaining six cubes labeled 1, 2, 3, 5, 6, 7 are indicated.

Figure 11: Case  $r = 3$ 

The centers of the  $8^3$  labeled 3-cubes suggested in the figure are original vertices of  $\Lambda^3$ . The convex hull of these  $8^3$  vertices constitutes a cutout of a 3-dimensional torus (flat in the sense of [4]) in which a 3-toroidal graph  $C_7 \times C_7 \times C_7$  is embedded, obtained by identification of (corresponding vertices in) opposite faces of the cutout, which happens to be a 3-dimensional cube of side lengths 8, that is: each side, or maximal lateral path of the cutout is a path of length 8. Then the distribution of the seven labels 1 through 7 yields a 1-perfect code partition of  $C_7 \times C_7 \times C_7$ , which illustrates the following corollary. By taking the inverse image of this partition through the canonical projection graph map  $\rho : \Lambda^3 \rightarrow C_7 \times C_7 \times C_7$ , a 1-perfect code partition  $\mathcal{S}_0$  is obtained in  $\Lambda^3$ . By reverting the label ordering along one of the coordinate directions, the enantiomorphic image of  $\mathcal{S}_0$  is obtained (through an  $(r - 1)$ -dimensional mirror), as well as the enantiomorphic image of  $\mathcal{S}_0$ , yielding a total of  $2(2r + 1)$  perfect codes equivalent to  $\mathcal{S}_0$ .

Likewise, an example for  $\Lambda^4$  leads to a 1-perfect code partition of the 4-toroidal graph  $C_9 \times C_9 \times C_3 \times C_9$ , where the component  $C_3$  corresponds to the third coordinate direction, with label differences  $\pm 3 \bmod 9$  between neighboring vertices along it. Theorem 8 and Corollary 9 generalize now as follows.

**Corollary 14**  $\Lambda^r$  admits a partition into  $2r + 1$  copies of  $\mathcal{S}_0$ . Moreover, the total number of perfect codes isomorphic to  $\mathcal{S}_0$  in  $\Lambda^r$  is  $2(2r + 1)$ .  $\square$

**Corollary 15** There exists an  $r$ -dimensional toroidal graph  $C_{m_1} \times \dots \times C_{m_r}$  having a 1-perfect code partition  $\mathcal{S}_0 = \{S_0^0 = S_0, S_0^1, \dots, S_0^{2r}\}$  if and only if  $m_i$  is a multiple of  $q / \gcd(q, i)$ , for  $i = 1, \dots, r$ . Each component code  $S_0^i$  of  $\mathcal{S}_0$  has cardinality  $m_1 \dots m_r / q$  and cannot be obtained by side identifications from 1-perfect codes in any  $r$ -dimensional parallelepiped grid graph. Identification of vertices in  $\Lambda^r$  with each common label  $i = 1, 2, \dots, q$  yields the quotient graph of the partition. This graph is  $K_q$ , that is the undirected Cayley graph of the cyclic group  $Z_q$  under the generator set  $\{1, 2, \dots, r\}$ .  $\square$

## References

- [1] B. F. AlBdaiwi and M. L. Livingston, *Perfect distance- $d$  placements in 2D toroidal networks*, Jour. Supercomput., **29** (2004), 45–57.
- [2] D. W. Bange, A. E. Barkauskas and P. J. Slater, *Efficient dominating sets in graphs*, Appl. Discrete Math, eds. R. D. Ringeisen and F. S. Roberts, SIAM, Philadelphia, 1988, 189–199.
- [3] N. Biggs, *Algebraic Graph Theory*, Cambridge University Press, 1993.
- [4] S. I. Costa, M. Muniz, E. Agustini, R. Palazzo, *Graphs, tessellations, and perfect codes on flat tori*, IEEE Transact. Inform. Theory, **50** (2004), 2363–2377
- [5] I. J. Dejter and A. A. Delgado, *Perfect domination in rectangular grid graphs*, J. Combin. Math. Combin. Comput., **70** (2009) 177–196.
- [6] M. R. Fellows and M. N. Hoover, *Perfect Domination* Australasian J. of Combinatorics, **3** (1991), 141–150.
- [7] W. F. Klostermeyer and J. L. Goldwasser, *Total Perfect Codes in Grid Codes*, Bull. Inst. Comb. Appl., 46(2006) 61–68.
- [8] J. Kratochvil and M. Krivánek, *On the Computational Complexity of Codes in Graphs*, in Proc. MFCS 1988, LN in Comp. Sci. 324 (Springer-Verlag), 396–404.
- [9] M. Livingston and Q. F. Stout, *Perfect Dominating Sets*, Congr. Numer., **79** (1990), 187–203.
- [10] R. Penrose, *Bull. Inst. Maths. Appl.*, **10** (1974), 266.
- [11] P. M. Weichsel, *Dominating Sets of  $n$ -Cubes*, J. Graph Theory, **18** (1994), 479–488.
- [12] J. L. A. Yebra, M. A. Fiol, P. Morillo and I. Alegre, *The diameter of undirected graphs associated to plane tessellations*, Ars Combinatoria, **20B**(1985), 159–171.

(Received 26 July 2007; revised 13 Nov 2007)